ELSEVIER

Journal of Structural Geology 29 (2007) 1695–1708

JOURNAL OF STRUCTURAL GEOLOGY

www.elsevier.com/locate/jsg

Thickness and spatial distribution of veins in a porphyry copper deposit, Rosia Poieni, Romania

Anne-Sylvie André-Mayer*, Judith Sausse

Nancy-Université, CNRS, UMR 7566 G2R, Géologie et Gestion des Ressources Minérales et Energétiques, B.P. 239, 54506 Vandœuvre-lès-Nancy Cedex, France

Received 3 May 2006; received in revised form 27 June 2007; accepted 28 June 2007
Available online 26 July 2007

Abstract

A statistical analysis of the vein thickness distributions of veins in the Rosia Poieni porphyry copper deposit, Romania, indicates that vein thickness data conform to a power-law distribution whereas the spatial distribution of veins follows a negative exponential law. A high clustering of the veins is indicated by both the spacing distribution and the C_v values. The similar vein densities observed at the open-pit scale are representative of a saturation level of vein nucleation. Differences in the spacing distribution and in the mean vein thickness are explained by different initial nucleation rates in the deepest and the lowest parts of the porphyry copper. The highly clustered organization of the system is explained by vein linkage processes during their growth and modification of the fluid pressure and local stress during the hydrofracturing. Published by Elsevier Ltd.

Keywords: Statistical analyses; Porphyry copper; Thickness; Spacing; Ore deposit

1. Introduction

A knowledge of the geometry of fracture networks is essential in several sub-surface geological domains (e.g. engineering for oil reservoirs, mining geology, and waste storage). Discontinuities such as fractures are potential sites for fluid circulation and have important implications for the hydraulic properties of rocks. The matrix permeability of igneous rocks is generally small and, consequently, the overall permeability is mostly controlled by fracture networks. Numerous papers have dealt with the description of natural vein or fracture networks occurring in various environments and focusing on statistical analyses. Several parameters have been studied, the main focus being on the spacing, thickness and length distributions of fractures. Velde et al. (1991) characterized the fractal distribution of fracture patterns in granites. Gillespie et al. (1993) compared different types of statistical and geometrical methods for the characterization of the spatial distribution of fractures in 1D, 2D and 3D. Johnston and Mc Caffrey (1996) established empirical relationships for vein shapes while Clark et al. (1995), Roberts et al. (1998, 1999) and Monecke et al. (2001) demonstrated that the use of statistical approaches is an important clue to understand the relationship between vein geometry and the mechanisms of vein formation. Other contributions based on natural fracture set studies in granites show that the connection of fracture systems is characterized by statistical laws deduced from the fracture extension distributions and that the fact that fluids follow preferential pathways within a fracture network (Bour et al., 2002; Bour and Davy, 1999; Ledésert et al., 1993a,b; Long and Witherspoon, 1985). A number of laws are commonly cited to characterize these distributions, the type of rock fragmentation, its development and maturity. Generally, log-normal, exponential negative or power law distributions are mentioned in the literature (Bonnet et al., 2001).

Johnston (1992) applied a statistical method to systematically characterize the veins that enhance productivity in existing mining areas and to assist the prospecting of new deposits.

* Corresponding author. Tel.: +33 03 83 68 47 56; fax: +33 03 83 68 47 01.
E-mail address: anne-sylvie.andre@g2r.uhp-nancy.fr (A.-S. André-Mayer).

0191-8141/$ - see front matter Published by Elsevier Ltd.
doi:10.1016/j.jsg.2007.06.010

Several other statistical analyses on vein thickness and spacing distributions have been conducted on mineralized vein systems by Sanderson et al. (1994), Mc Caffrey and Johnston (1996), Roberts et al. (1998, 1999), Loriga (1999), Brathwaite et al. (2001) and Monecke et al. (2001). Hence, statistical studies of the geometrical parameters of vein or fracture systems represent a useful way to characterize the spatial distribution and the hydraulic and metallogenic behaviour of fracture networks.

This paper outlines a statistical study of a vein system in a mineralized stockwork from the Rosia Poieni porphyry copper deposit, Romania (Fig. 1). The spatial and thickness distributions of the veins constituting the stockwork are examined and compared with similar distributions proposed in the literature. The evolution of the vein architecture at the open-pit scale is described and the mechanisms responsible for the stockwork formation are discussed.

2. Geological setting

2.1. The Apuseni Mountains and the Rosia Poieni porphyry copper deposit

The southern part of the Apuseni Mountains (West Romania) shows a variety of mineral occurrences (Cioflica et al., 1973; Ianovici et al., 1977; Borcos et al., 1983; Udubasa et al., 1992; Heinrich and Neubauer, 2002) related to Neogene volcanic activity (Lemne et al., 1983; Pecksay et al., 1995; Rosu et al., 1997; Alderton et al., 1998).

The Rosia Poieni porphyry copper deposit, the largest porphyry copper in the Apuseni Mountains, belongs to the metallogenic district of Bucium-Baia de Aries (Fig. 1). The basement here consists of Pre-Mesozoic metamorphic rocks intruded by magmatic bodies and covered by pyroclastics of variable composition (Fig. 1). Two types of igneous rocks, both characterized by intense hydrothermal alteration, are exposed in the open-pit. The host rocks, the Poieni andesite, are intruded by a subvolcanic body characterized by a porphyritic texture, the Fundoaia microdiorite (Fig. 2). Ionescu (1974), Ionescu et al. (1975) and Bostinescu (1984) carried out a mineralogical and petrographic study of the rocks from the Rosia Poieni area. They identified the disseminated character of the copper mineralization and a zoned pattern of alteration. Recent studies (Milu, 1999; Milu et al., 2004) have shown that the Fundoaia subvolcanic body and the Poieni host rocks are characterized by strong hydrothermal alteration spatially related to the Fundoaia intrusion.

Fig. 2 presents a schematic reconstruction of the Rosia Poieni volcanic structure and shows the concentric pattern of

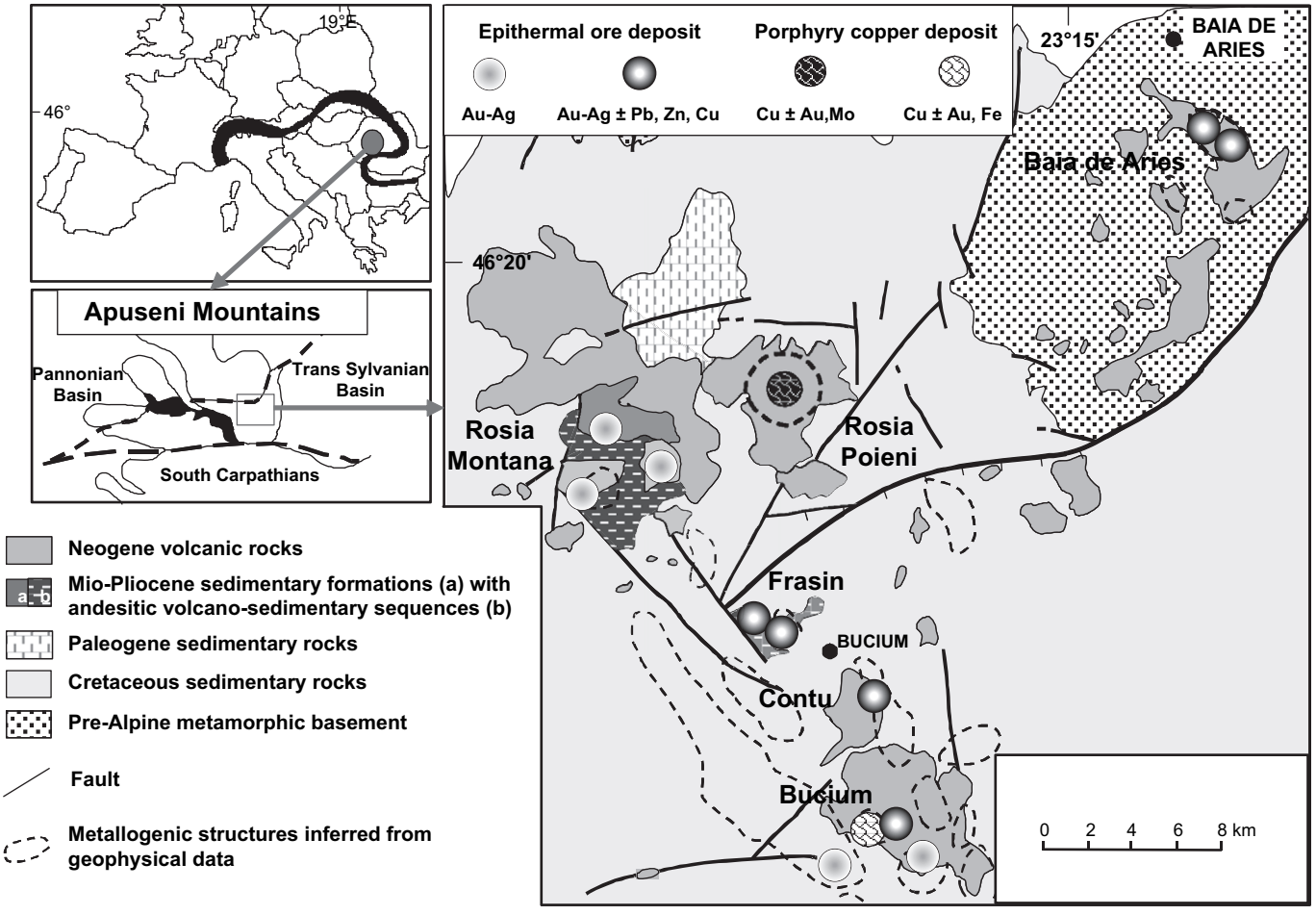

Fig. 1. Geological map of the Bucium-Baia de Aries metallogenic district located in the Apuseni Mountains, Romania (modified from Borcos et al., 1983).

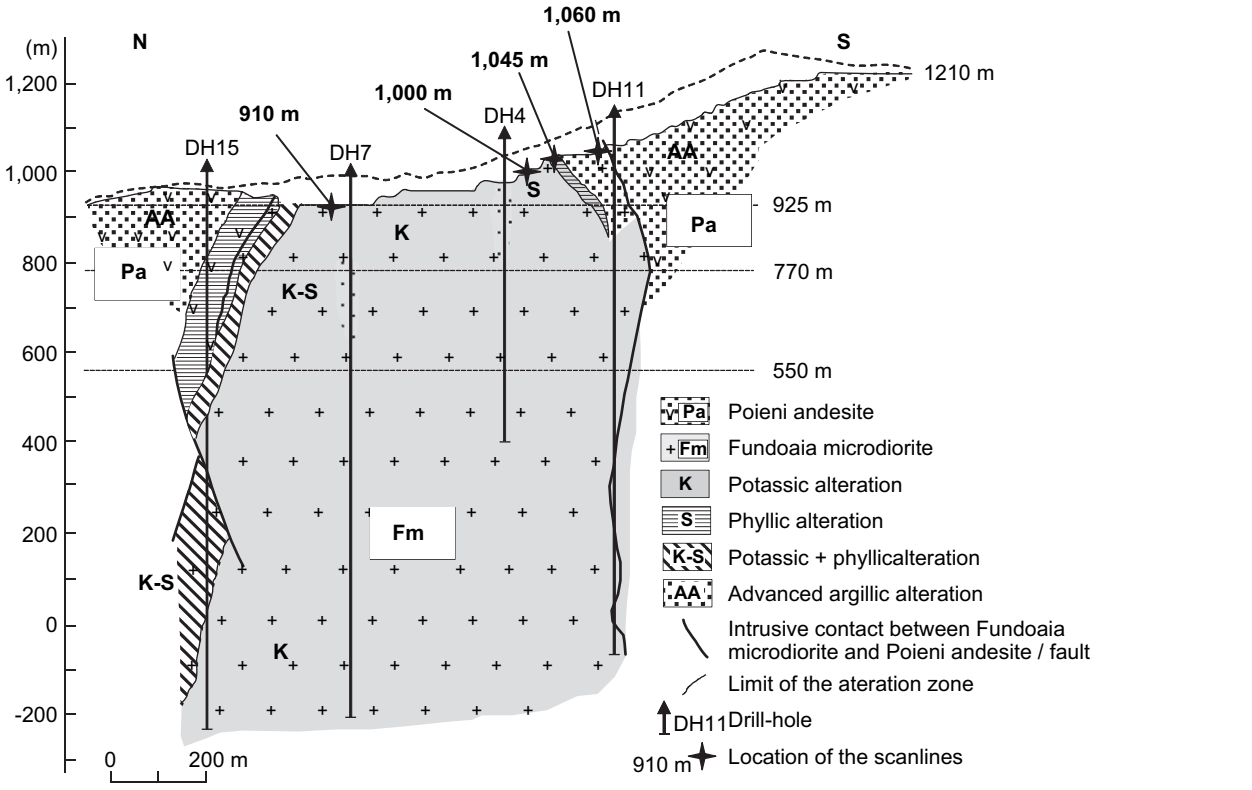

Fig. 2. North–south cross-section of the Rosia Poieni open-pit (reconstructed from Ionescu (1974) and Milu et al. (2004)) showing the porphyritic intrusion and host rocks, alteration types and zones. The location of the four scanlines (900, 1000, 1045 and 1060 m) is indicated with stars.

the hydrothermal alteration from a potassic core to a well-developed advanced argillic zone (Milu et al., 2004). The main high-grade zone (>0.6% Cu) is located in the central part of the intrusion (Milu et al., 2004). Outside the potassic limits, the copper grade decreases to 0.1% Cu, except in zones where a phyllitic alteration is superimposed on a potassic alteration (Fig. 2). The upper part of the Rosia Poieni structure displays an advanced argillic alteration and is barren (<0.05% Cu). Gold occurrences, higher than 0.02 ppm Au (lower limit of detection) are restricted to the potassic (±phyllic) zones, but do not exceed a mean value of 0.5 g/t Au (www.gabriel-resources.com and Milu and co-workers, 1999, 2004). At the present day the open-pit is on standby, but the reserves are estimated to be around 350 Mt with an ore grading of 0.36% Cu and 0.29 g/t Au (Borcos et al., 1998).

The mineralization comprises pyrite, chalcopyrite, magnetite, hematite, molybdenite and bornite with subordinate tetrahedrite–tennantite, enargite and digenite and minor pyrrhotite, sphalerite, galena, covellite and chalcocite. Chalcopyrite is the dominant hypogene copper mineral. The mineralization is pervasively disseminated within the altered rock and within the veins and fractures associated in a well-developed stockwork (Figs. 2 and 3) that is best developed in the potassic zone.

2.2. Data collection

The present vertical extent of the open-pit exposure is 300 m (between altitudes of 910 and 1210 m; Figs. 2 and 4).

Four horizontal sampling lines were chosen in the open-pit at different altitudes (910, 1000, 1045 and 1060 m; Fig. 4). In most mineral exploration situations (trenches, boreholes, drifts, etc.) only this type of 1D sampling is allowed, despite the 3D organization of both individual veins and networks (Park and West, 2002; Peacock et al., 2003). Moreover, existing methods allowing a 2D data analysis are still immature and no satisfactory method yet exists to analyze 3D spatial data (Gillespie et al., 1993; Pickering et al., 1995).

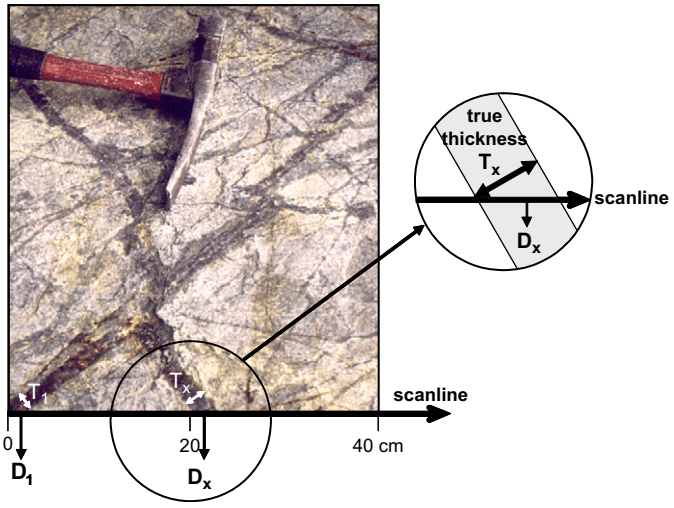

Fig. 3. Stockwork organization and method of sampling along each scanline: distance from the beginning of the scanline (D_1, … ,D_x, …), true thickness (T_1, …, T_x, …), strike, dip and mineral assemblage of each vein are plotted.

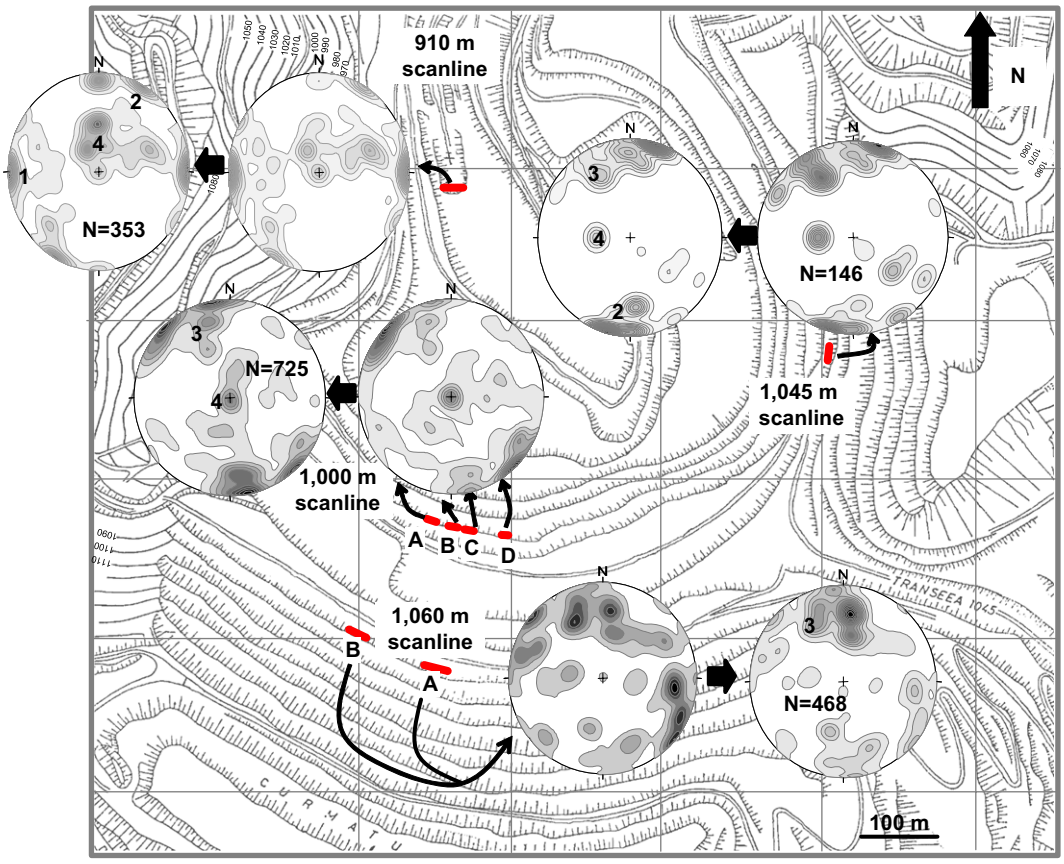

Fig. 4. Topographic map of the Rosia Poieni open-pit. Each stope is 15 m high. The fracture orientation plot (poles to planes) is described using two stereographic projections (Schmidt net) for each of the four scanlines. One stereonet presents the raw data whilst the other presents the same data adjusted using the Terzaghi correction (see text for details). Four preferential orientations of veins are identified, N–S (family 1), NW–SE (family 2), NE–SW (family 3) and sub-horizontal (family 4). *N* is the number of fractures sampled for each scanline.

Three of the sampling lines are oriented in an approximately E–W direction (altitudes 910, 1000 and 1060 m), whereas the fourth is oriented N–S (altitude 1045 m; Fig. 4). The 1060 m scanline is located close to the contact between the intrusive body of Fundoaia and the host andesite of Poieni marked by the onset of the argillic alteration (Fig. 2). For each scanline and each vein, the intersection distance (spacing) between the vein and the scanline was measured and information such as thickness, strike, dip and vein mineral assemblage were collected (Fig. 4; Table 1). Vein counts range from 146 to 725 over lines of lengths from 7.9 to 14.4 m leading to a database of about 1700 fractures (Figs. 3, 4; Table 1).

This substantial database is considered to exceed the threshold of sampling lines that is required in order to obtain stable statistical results. Indeed, this threshold has varied considerably among different authors: thus Pickering et al. (1995) and Mc Caffrey and Johnston (1996) used 50 values, whilst Berkowitz and Adler (1998) examined 100 data for simple cases (constant fracture size). About 200 values were recommended by Priest and Hudson (1976) and Bonnet et al. (2001). In this study, the data sets, ranging from 146 to 725 values, are considered to be robust enough for statistical analyses.

The 1000 and 1060 m scanlines are not continuous due to unsafe access conditions caused by presence of screes or strong weathering. They are thus divided, respectively, into four and two sections (Table 1). The recorded minimal value of vein thickness is 1.0 mm. Vein spacings are measured from vein centre to vein centre (Fig. 3).

3. Method

3.1. Vein thickness distribution

Details of the vein thickness distributions are fully documented by numerous authors such as Velde et al. (1990, 1991), Barton and Zobach (1990), Merceron and Velde (1991), Ledésert et al. (1993a,b), Sanderson et al. (1994), Clark et al. (1995), Genter et al. (1995), Johnston and Mc Caffrey (1996), Mc Caffrey and Johnston (1996), Roberts et al. (1998, 1999), Loriga (1999) and Monecke et al. (2001). Generally, in the case of non-stratabound vein systems (Gillespie et al., 1999), the cumulative frequency plot of the vein thickness follows a power law distribution given by:

$$N_T = CT^{-D} \quad (1)$$

where N_T is the cumulative number of veins with a given thickness $\geq T$, D, the slope of the log–log plot and C, the frequency of veins $\geq$unit size. In this case, a log–log plot of N_T

Table 1
Database acquired on the Rosia Poieni stockwork with indications of length, number of data, vein density and strain for each scanlines

Scanline (m)	Section	Length (m)	Number of data		Density N/m (m^{-1})	Strain (%)
910	–	12.7	353		27.5	12.2
1000	1	11.3	213	725	18.8	7.0
	2	14.4	205		14.2	
	3	10.2	219		21.5	
	4	7.9	88		11.2	
1045	–	11.0	146		13.3	3.4
1060	1	13.2	210	468	15.9	8.3
	2	8.1	258		31.7	

The 1000 and 1060 m scanlines are not continuous because of access problems due to the presence of screes or strong weathering and are thus, respectively, divided in four and two sections.

versus T gives a linear trend with a slope corresponding to the exponent D of Eq. (1). This exponent is commonly associated with the fractal dimension of the distribution. It is important to point out that this law is called "fractal" in relation to its statistical distribution even if there is no implication of scale in the sense defined by Mandelbrot (1983). Furthermore, in natural media, power law relationships can be limited by physical length scales that form the upper and lower limits to the scale range over which they are valid (Bonnet et al., 2001).

In this study, a conventional cumulative frequency versus length distribution is used which plots the cumulative number of veins (N_T) with thicknesses greater than a given value (T). N_T is normalized in respect to the scanline lengths (m) (Table 1) in order to allow a comparison between the different pit levels.

3.2. Spatial distributions of veins

The analytical method used to characterize the spatial distribution of veins is the spacing population technique. This technique determines the cumulative frequency distribution of the intersection distance between adjacent veins and the scanline (Harris et al., 1991).

Log–log plots of the spacing distributions are used which plot the cumulative number of veins (N_T) with spacing greater than a given value S (Harris et al., 1991; Gillespie et al., 1993). Other characterizations of the fracture spacing distributions exist in the literature such as interval counting (Smalley et al., 1987; Velde et al., 1991) or fracture number interval techniques (La Pointe, 1988). However, the spacing population technique is currently described as the most simple and efficient method to characterize vein populations in terms of their spacing distributions.

Another suitable measure of the variability of the spacing is given by the coefficient of variation C_v (Cox and Lewis, 1966; Gillespie et al., 1999, 2001) which is defined as:

$$C_v = \frac{\sigma_s}{\mu_s} \quad (2)$$

where σ_S is the standard deviation of the spacing between adjacent veins along the scanline, and μ_S, the mean value of the spacing.

This parameter is used to determine the degree of clustering of points along a line. Clustered veins are characterized better by strongly variable spacings than random ones implying a C_v higher than 1.0. More regularly distributed (or anticlustered) veins show a different C_v with values lower than 1.0. A perfectly regular set of veins can be represented by a spacing standard deviation of 0 and therefore C_v will be equal to 0. Hence, the C_v statistical parameter describes the full range of spatial distributions from anticlustering to clustering. The evolution of this parameter as a function of a threshold thickness can also be described. Depending on the type of spacing distribution, this evolution will be different. For example, a power-law distribution will have a C_v decreasing with increasing threshold thickness, which is consistent with the smaller veins being systematically more clustered than the larger ones.

4. Stockwork geometry and vein density

Table 1 shows that the vein densities have similar magnitudes for the four scanlines with 27.5, 15.6, 13.3 and 21.6 veins per meter for the 910, 1000, 1045 and 1060 m scanlines, respectively.

Anisotropic orientations of the veins constituting the stockwork are observed and described in Fig. 4. The geometry of the vein network is characterized by four preferential orientations: N–S (family 1), NW–SE (family 2) and NE–SW striking veins (family 3) and a sub-horizontal set (family 4). These families are not observed everywhere along the scanlines and their occurrences are indicated in Table 2 and Fig. 4. The 1060 m level shows a more widespread distribution of vein orientations compared to the others.

To assure that this anisotropic system is truly representative of the vein network and independent of the scanline orientation, the Terzaghi correction (Terzaghi, 1965) was applied. This correction applies a weighting, the number of fractures cut by the scanlines with respect to their orientation. The angle δ between the normal of the fracture plane and the scanline is used to calculate the probability for a fracture plane to intersect the scanline or not. A fracture characterized by a δ angle of 0° has the highest probability of intersection because its plane is perpendicular to the scanline (Eq. (3)). By contrast, the lowest probability of intersection is obtained when the fracture is parallel to the scanline and therefore characterized by a δ angle of 90° (Eq. (3)). Any sampling will be biased

Table 2
Occurrence for each scanline of the four different families of vein orientations observed in the open-pit and mean and standard deviations of the vein thicknesses

Scanline (m)	F1 (N–S)	F2 (NW–SE)	F3 (NE–SW)	F4 (subvertical)	Mean thickness (mm)	Standard deviation thickness
910	X	X	–	X	4.46	9.48
1000	–	–	X	X	4.20	6.63
1045	–	X	X	X	2.54	5.94
1060	–	–	X	–	3.79	8.20

because of the scanline directionality and the resulting database contains a lower amount of fractures than are actually present. This problem of under-sampling can be solved by the Terzaghi correction which assigns to each fracture plane i, a weighting factor W_i corresponding to the probability of intersection with the scanline (Eq. (3)).

$$W_i = \frac{1}{\cos(\delta_i)} \tag{3}$$

where δ_i is the angle between the normal of the fracture plane and the scanline.

The problem is that the δ angle ranges from 0° to 90° and when they are close to 90°, Eq. (3) produces very large and artificial values of W_i. This mathematical problem can be solved using a normalized weighting factor W_{ni}. The normalization presented in Eq. (4) forces the initial number of sampled fractures to remain constant:

$$W_{ni} = \frac{W_i \times N}{N_W} \tag{4}$$

where W_i is the initial weighting factor, N, the number or fractures and N_W, the summation of $W_i : N_W = \sum_{i=1}^{N} W_i$.

Stereographic projections modified by applying the Terzaghi corrections are presented in Fig. 4 (black stars on Fig. 4) and compared to the raw orientation data. The stockwork geometry still shows, even with this correction, a markedly anisotropic pattern and preserves the main and recurrent directions of fractures despite its hydraulic fracturing origin. These orientations are consistent with the E–W extensional tectonic regime that occurred in this area during the formation of the porphyry copper deposit. However, regarding the spreaded orientation of the veins, it is not obvious, whether a predominant influence of the tectonic regime or of the hydraulic fracturing is responsible.

The extensional longitudinal strain has been estimated for each level. The data are presented in Table 1. The degree of deformation is higher in the lower level +910 m compared to the upper ones.

5. Thickness distribution

The plots of cumulative frequency of vein thickness for each scanline show that the thickness distributions follow power-law relationships (Fig. 5A). The identification of a specific theoretical distribution law to characterize the raw data distribution can be ambiguous because a biased power-law distribution can resemble a log-normal one. A simple visual examination of the plot is not sufficient, especially in this case where the size range of thicknesses is limited to two orders of magnitude (Fig. 5A). It can be easily seen that the theoretical log-normal and negative exponential distributions (dotted lines in Fig. 5A), respecting the mean and the standard deviation of each distribution, do not really match the field data whereas the theoretical power-law (continuous lines on Figs. 5A and B) provides a better fit. Furthermore, correlation coefficients R between the raw and theoretical data for the power law are systematically higher than the other types of statistical distribution (R higher than 0.96 in Fig. 5A).

However, some deviations from the expected trends occur on the left-hand and right-hand sides and are typical of most natural data sets (Sanderson et al., 1994; Mc Caffrey and Johnston, 1996; Roberts et al., 1998; Roberts et al., 1999). They are generally attributed to two types of truncation: the under-sampling of the thinnest veins and the low probability of intersection of the thickest veins with the scanline (Barton and Zobach, 1990; Pickering et al., 1995). Corrections have been applied to avoid these two types of deviation. For the left-hand side, the correction proposed by Mc Caffrey and Johnston (1996) and Roberts et al. (1998) was applied by removing all small thickness values below a certain T_L from analysis. For the right-hand side (taking into account the preceding left-hand side correction), the method proposed by Pickering et al. (1995) and corrected by Monecke et al. (2001) was applied. This correction procedure predicts the amount of thick veins that cannot be intersected by the scanline. The cumulative number of the thicker veins showing a right-hand fall-off is simply assumed to be too small and has to be corrected with the addition of an unknown N_R quantity of missed thicker veins. A corrected cumulative number N_C can be calculated according to $N_C = N + N_R$. N_R is chosen to minimize the deviation of the $\log N_C$ versus $\log T$ curve from a straight line. Table 3 presents the values of T_L and N_R that best respect this criterion. T_L is equal to 1 mm for all the scanlines and N_R is very low (≤ 1). These low values of T_L and N_R indicate that the length of the scanlines is pertinent and involves no bias of sampling for the thicker veins. The corrected vein thickness distributions are presented in Fig. 5B.

In each scanline, the veins have been considered all together whatever their orientation or mineralogical fill. The formation of the vein system by hydraulic fracturing makes it difficult to separate each orientation set. However, some tests have been carried out to see if this indiscriminate sampling has an effect upon the fractal character of the thickness distribution. The results are presented in Fig. 6. The fractal character of the distribution is still observed when veins are discriminated into different orientation sets (Fig. 6A). In the same way, and even if no chronological relationships have been established between the different veins, the corrected thickness distributions between veins hosting only quartz and/or pyrite (QP) and those hosting at least one copper mineral (chalcopyrite, bornite and/or enargite) (Cu) have been compared. Fig. 6B shows the result for the example of the +1000 m profile: Cu veins are characterized by a lower fractal dimension than the QP ones, and this can be directly linked to the higher density of thick Cu veins.

The fractal character of the thickness distributions existing for each scanline is thus obvious. This conclusion supports the hypothesis that non-stratabound vein arrays are characterized by power-law thickness distributions (Gillespie et al., 1999). This type of distribution has already been described in the literature in other hydrothermal vein-style deposits by Sanderson et al. (1994), Gross and Engelder (1995), Khrul (1994), Clark

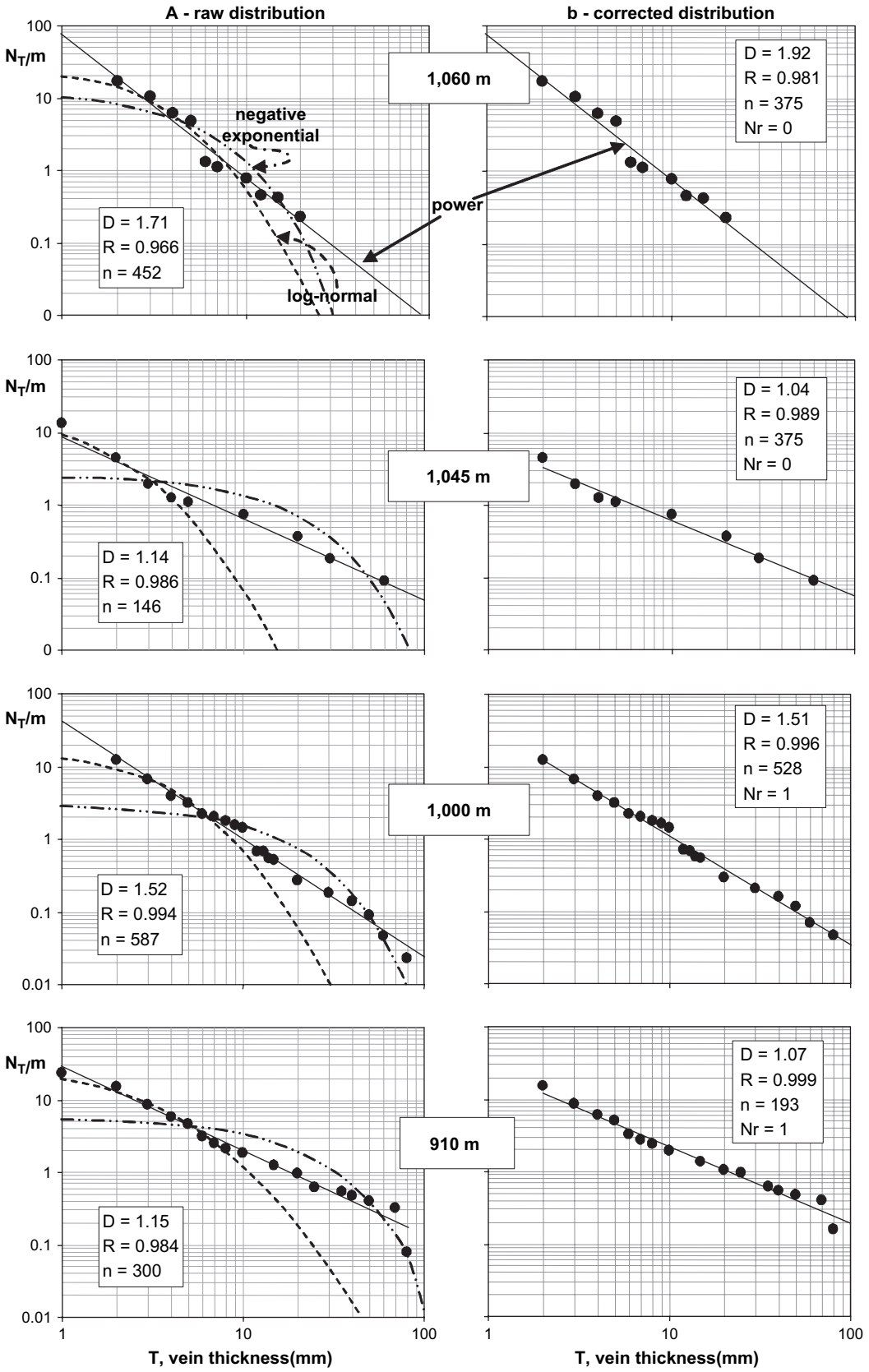

Fig. 5. Log−log plot of the cumulative normalized frequency N_T/m of veins versus the thickness classes T for the different scanlines. (A) Raw distributions (black circles) compared with a theoretical power law (continuous line), log−normal (dashed line) and negative exponential (dotted line) distributions, drawn with the knowledge of the mean and the standard deviation of each distribution. (B) Raw distributions (black circles) compared with a theoretical power law (continuous line), log−normal (dashed line) and negative exponential (dotted line) distributions, drawn with the adjusted distributions (black circles) after the application of left- and right-hand side corrections (see text and Table 2 for details). D is the fractal dimension, n the number of veins and Nr the additional amount of veins used for the right-hand side correction. R is the correlation coefficient between the raw and theoretical power law data with R_{exp} for the exponential negative distribution and R_{pl} for the power-law distribution one.

Table 3
Summary for each scanline of T_L and N_R values used for the left- and right-hand side corrections, fractal dimensions, correlation coefficients between the raw and theoretical power-law data for the thickness distributions

Scanline (m)	Correction of sample bias		Fractal dimension	Correlation coefficient
	T_L (mm)	N_R (mm)	D	R (power-law)
910	1	1	1.07	0.99
1000	1	1	1.51	0.99
1045	1	0	1.04	0.99
1060	1	0	1.92	0.98

et al. (1995), Jonhston and Mc Caffrey (1996), Mc Caffrey and Jonhston (1996), Gillespie et al. (1999), Roberts et al. (1999), Loriga (1999) and Monecke et al. (2001). This study is the first to show, however, that a porphyry vein system constituting a stockwork and generated by a hydrofracturing process, conforms to a power-law relationship.

The fractal dimension D increases from 1.1 for the 910 m scanline to 1.9 for the 1060 m scanline (Table 3, Fig. 5). The whole field database is sampled in the same rock lithology, the Fundoaia andesite (Fig. 2). Thus, these fluctuations in fractal dimension do not reflect lithological variations in the stockwork host rock (Brathwaite et al., 2001).

6. Spacing distribution

The intersection distances between adjacent veins (spacing S) are presented in a log–log diagram plotting the cumulative number of veins (Ns) with spacings greater than a given value S versus the spacing classes S (Fig. 7). All the levels show negative exponential distributions as shown by the high correlation coefficients R (Fig. 7). The spacing distribution of the 910 m level is more ambiguous: the fractal distribution seems to be more adapted, but the value of $D > 1$ is incoherent with a spatial distribution along a line. As for the thickness distribution, tests have been carried out to see if the indiscriminate sampling whatever the orientation or mineralogical fill has any effect upon this negative exponential distribution. The results are presented in the Fig. 6 for the 1000 level. For the two main orientation sets, the negative exponential character is still evident.

These types of distribution were previously observed in this type of massive and non-layered crystalline rocks (Cowie et al., 1994; Gillespie et al., 1999; Brathwaite et al., 2001). Brooks et al. (1996) performed an analysis of the spacing distribution of faults observed at the scale of a crystalline rock body (porphyry copper deposit, El Teniente, Chile) and demonstrated that the spatial distribution of the system follows a negative exponential law.

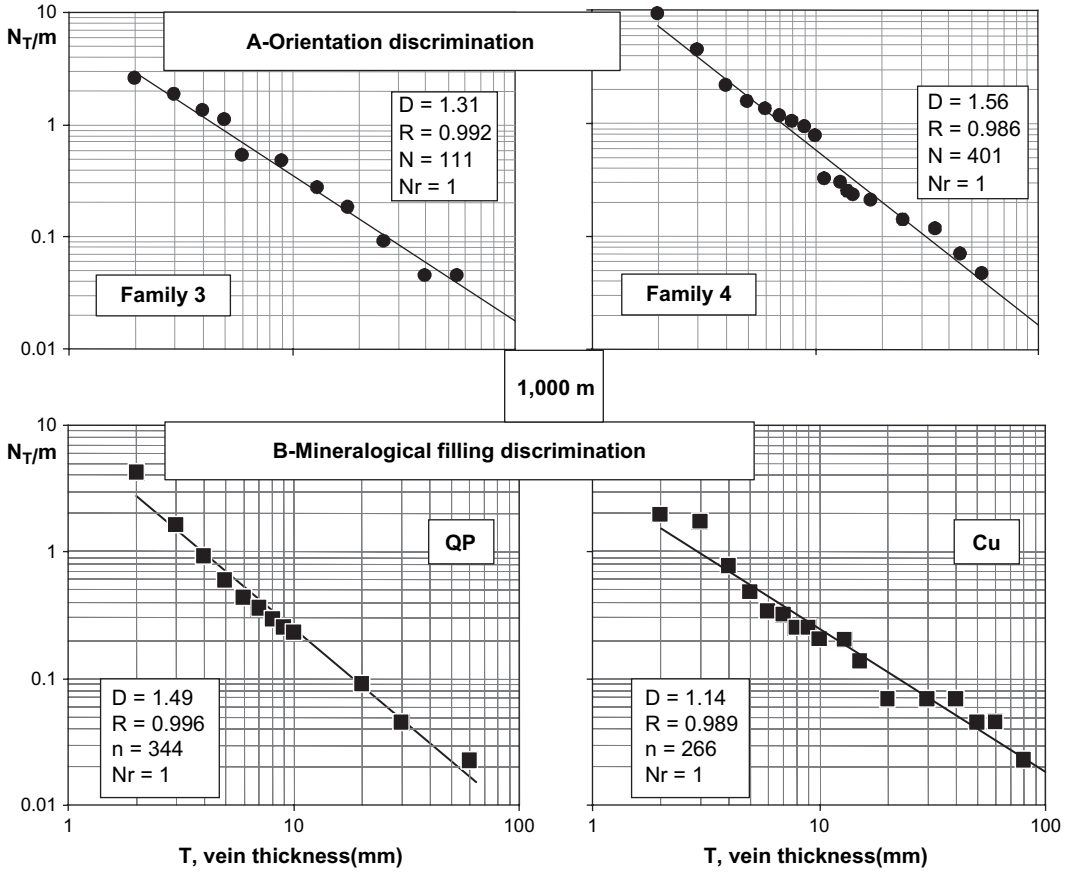

Fig. 6. Log–log plot of the cumulative normalized frequency N_T/m of veins versus the thickness classes T for the 1000 m level with discrimination of the vein sets in terms of (A) vein orientations and (B) mineralogical filling. There are corrected distributions (black circles) after the application of left- and right-hand side corrections (see text and Fig. 5 for details).

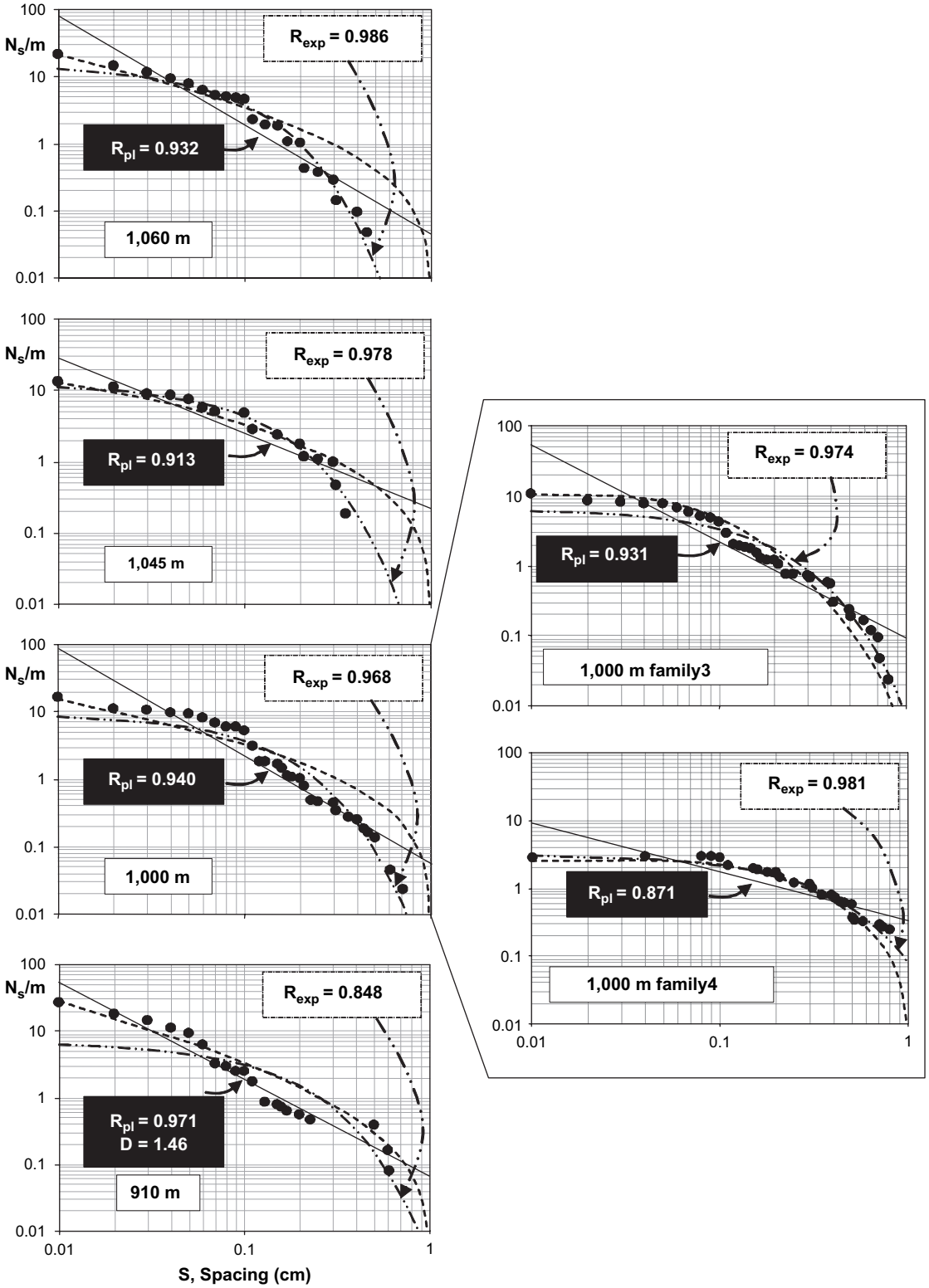

Fig. 7. Log–log plot of the cumulative normalized frequency N_S/m of veins versus the spacing classes S for the different scanlines. The raw distributions are plotted with black circles and are compared with theoretical power law (continuous line), log–normal (dashed line) and negative exponential (dotted line) distributions, drawn with the knowledge of the mean and the standard deviation of each distribution. D is the fractal dimension corresponding to the power law adjustment of the 910 m scanline. Two theoretical distributions can fit to the raw data: R_{pl} and R_{exp} are the correlation coefficients for the theoretical power law and negative exponential data, respectively. For the +1000 m profile, spacing distributions of sets with different orientation have been compared.

The C_v coefficient has been calculated for each scanline. All the values are >1 and indicate a clustered organization for the veins (Fig. 8). The 910 m level shows the highest value of C_v which indicates a stronger clustering than the other scanlines. These C_v values are similar to those estimated for other non-stratabound mineralized systems (Gillespie et al., 1999; Mc Caffrey and Johnston, 1996; Brooks et al., 1996).

7. Discussion

7.1. Vein thickness and vein growth mechanism

Two models are currently proposed to explain the mechanisms responsible for the formation of veins characterized by a power-law thickness distribution.

Stochastic models suggest that this type of distribution can be produced by a constant nucleation of veins in the media (Clark et al., 1995) with the assumption of a time-averaged growth rate proportional to the size of the structure (Ijiri and Simons, 1977). An analytical formulation of such a model has been proposed by Monecke et al. (2001) with a fractal dimension D, function of the nucleation rate (α) and the growth rate (β) with $D = f(\alpha/\beta)$. In this case, a high nucleation rate yields a higher fractal dimension D, i.e. a vein population dominated by a high relative proportion of thin veins, whereas a large constant growth rate (β) produces a small fractal dimension D, i.e. a vein population that contains a high relative amount of thick veins.

In *percolating cluster models* proposed by Sanderson et al. (1994), Roberts et al. (1998, 1999) and Cox (1999), the veins are assumed to grow with respect to some conditions and especially a growth rate function proportional to the size of the vein. The main difference with the stochastic model is that linkage of veins is considered to be essential in the formation of a pathway across the vein network, with wider veins being more susceptible to linkage and more likely to form connected pathways compared to thinner ones.

In both models, the fractal dimensions of the thickness distributions reflect directly the mechanisms responsible for the formation and evolution of the vein system. For Roberts et al. (1998), isolated veins will be dominated by small lengths and thicknesses whereas connected-systems of veins will be dominated by wider and more extended veins. In this case, a low D value will express a well-connected network which favors the percolation of mineralizing fluids.

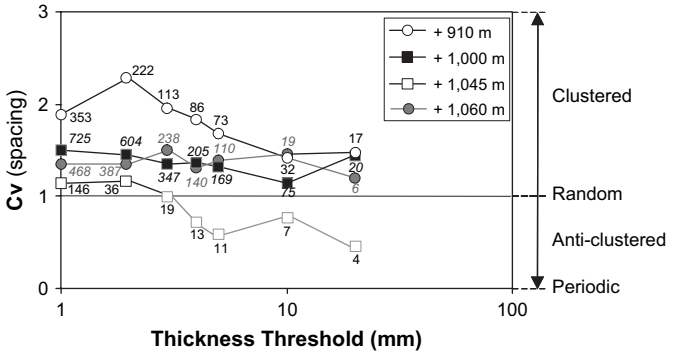

Fig. 8. Coefficient of variation (C_v) versus the thickness threshold for the four scanlines. The evolution of the C_v values observed for the 1045 scanline seems to be biased because of a lack of veins with apertures larger than 3 mm at this level of the open-pit.

The analytical formulation of Monecke et al. (2001) considers that D is dependent on the ratio between nucleation rate (α) and growth rate (β) and proposes that the formation of mineralized veins occurs at particularly low α/β ratios whereas weakly mineralized and barren veins are formed at higher α/β ratios.

In this study, D values increase from the bottom to the top of the porphyry system. A first conclusion could be that the nucleation rate α increases from the top to the bottom of the pit, but this is inconsistent with the observed data, since the vein density values are similar for all the scanlines (Table 1). A second possibility is that the growth rate β decreases from the bottom to the top. This implies a theoretically higher proportion of wide veins for the lower part of the system. Indeed, the mean thicknesses of veins decrease from 4.46 to 3.79 mm, respectively, for the 910 m and the 1060 scanlines (Table 2). It is proposed, therefore, that the evolution of the D parameters in this porphyry system is linked to changes in the growth rate of existing vein structures rather than to the nucleation of new ones. The evolution of D values observed in this study seems therefore to be independent of the nucleation rate.

Given the low D values observed for the lower levels of the mine, it is suggested that mechanisms of linkage are likely to be important so that the percolating cluster model proposed by Sanderson et al. (1994), Roberts et al. (1998), Cox (1999) and Roberts et al. (1999) is an appropriate way to describe the evolution of the vein distribution in this porphyry copper deposit.

It ought to be possible to describe this phenomenon by a comparative study of the thickness to length ratios of each vein as thicknesses are considered to be proportional to the lengths of the veins (Johnston and Mc Caffrey, 1996). The linkage process should disturb this relationship – as shown by Cartwright et al. (1995) – but as the lengths of the veins cannot be measured in this study, this analysis is not possible.

The formation of the vein network by a hydrofracturing mechanism implies the presence of high fluid pressure exsolved fluids (Hedenquist and Lowenstern, 1994; Bodnar, 1995) and a resulting high nucleation rate α, leading to a high density of veins. This mechanism could explain the higher D values (up to 1.92, Table 3) observed in this study compared to other types of hydrothermal deposits (Sanderson et al., 1994; Johnston and Mc Caffrey, 1996; Mc Caffrey and Johnston, 1996; Roberts et al., 1999; Loriga, 1999; Monecke et al., 2001). The high values of D observed in this system indicate also that the vein system is dominated by thinner veins as already described in Clark et al. (1995) and Roberts et al. (1999).

7.2. Vein spacing distribution and vein growth mechanism

The spacing distribution is ambiguous for the +910 m level, whereas the other levels indicate obvious negative

exponential distributions. Gillespie et al. (1993) described how under-sampling of the thinnest veins could affect the spacing distribution. Where the smallest veins with power-law thickness distribution are not detected, the spacing data are inevitably degraded and will not generate power-law distributions (Gillespie et al., 1993). The non-consideration of the smallest veins in the studied arrays leads to an under-sampling and to a degradation in the first part of the cumulative frequency curves. The correlation between the raw data and the theoretical power-law curves is therefore bad and the distribution cannot be interpreted as power-law. The frequency curve morphology conforms, in fact, better to the theoretical case of the exponential negative law. In this study, the sampling method is identical for the four scanlines. The sampling bias could theoretically influence the distributions, but should do so in a similar manner.

A clustered organization of veins, shown by the presence of either a power law or negative exponential spacing distributions, indicates that the nucleation locations of the veins (or fractures) are likely to be interdependent (Gillespie et al., 1993).

The interaction process tested numerically by Rives et al. (1992) suggests that the joint set development is controlled by the spatial distribution of the initiation points, the size of interaction zones, the initiation and propagation criteria of the joint sets and the stage of evolution. In this model, no fracture can nucleate at less than a certain limiting distance from any other fracture and the area available for joint initiation decreases with the cumulative length of the joints until no more freedom for the final fractures exists. The final stage of development is referred to by Narr and Suppe (1991) as the "saturation level".

If the fracture saturation level and therefore maximum density are reached, the strains developed in the rock body are expressed by the opening of pre-existing fractures rather than the nucleation of new fractures. In the porphyry case, homogeneous values of vein density can illustrate such a state of saturation. Hence, growth of the fractures occurs until a percolation threshold is reached. The actual vein system observed in the porphyry constitutes the final stage of the network development. This fact implies that the initial nucleation rate could not be identical for all the levels (Fig. 9) and that the time to reach the saturation level should be shifted in time for the different levels.

However, Simpson (2000) has shown that the modifications of the fluid pressure and local stresses during hydrofracturing can have an important effect on the resulting fracture spacing distribution. The fluid pressure drop within the fracture plane during failure perturbs the local stresses and the fluid pressure regime in the surrounding rock in a zone extending over approximately two fracture lengths. In contrast to the previous studies by Rives et al., 1992 and Gillespie et al. (1992, 1993), numerical simulations demonstrate that the nucleation of new fractures is located in the vicinity of the pre-existing fractures (Simpson, 2000).

The porphyry system is considered to be formed by a hydrofracturing process and therefore in this porphyry environment, veins must nucleate preferentially near pre-existing ones. This mechanism explains the existence of clustered vein systems, at the open-pit scale, in this case as shown by C_v values systematically higher than 1 (Table 4, Fig. 8).

The fluid pressure affects the bottom part of the vein system more strongly than the upper part and the degree of clustering

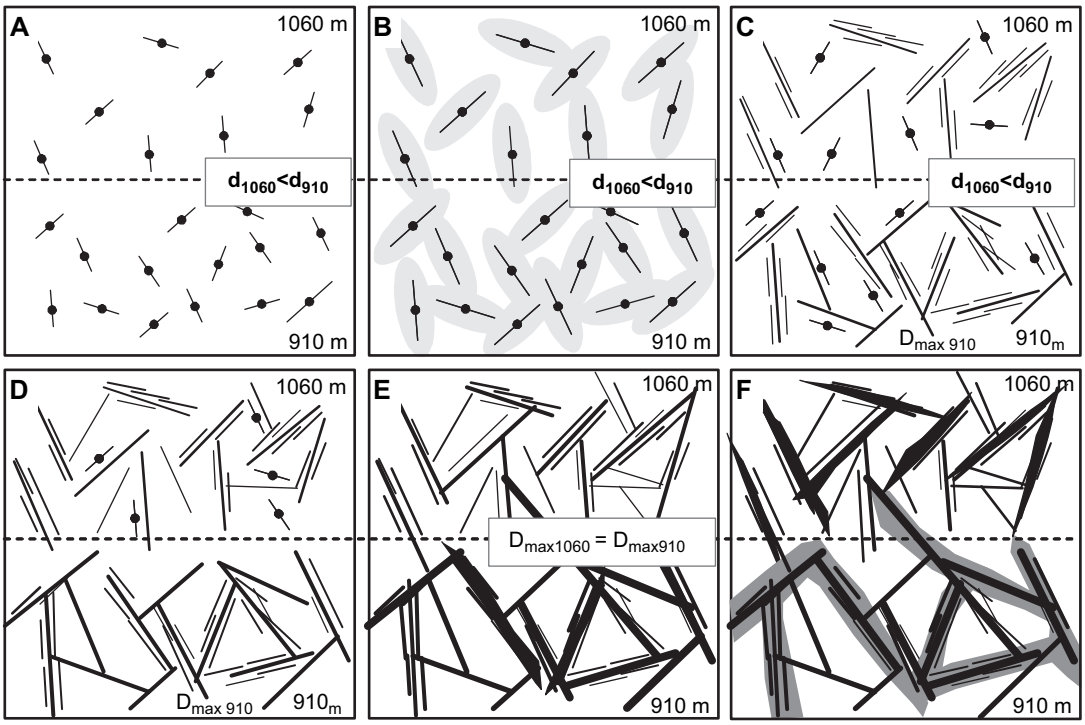

Fig. 9. Conceptual model for the formation and evolution in time and space of the vein network in the Rosia Poieni porphyry copper. See text for details.

Table 4
Mean spacings, standard deviations and C_v values characteristics of the four scanlines

Scanline (m)	Mean spacing (m)	Standard deviation spacing	Coefficient of variation, C_v
910	0.038	0.073	1.92
1000	0.067	0.100	1.49
1045	0.078	0.089	1.14
1060	0.05	0.10	1.31

is therefore different with more clustered veins in the bottom part compared to the upper part of the hydrothermal system.

7.3. Stockwork development and mineralization processes

The evolution of the fractal dimension D characterizing the distribution of the vein thicknesses, as a function of the mineralization rate has been outlined by Sanderson et al. (1994) and Roberts et al. (1998, 1999). These authors propose that a low D value is characteristic of well connected-systems which can thus develop favourable and substantial percolation rates of ore fluids. Wilkinson and Johnston (1996) show that a clear relationship exists between the clustered organization of veins and gold precipitation suggesting that the mechanical and the chemical development of the veins are strongly related. Indeed, in the case of the porphyry copper stockwork studied in this paper, the vein clustering seems to play a major role in the mineralizing processes.

As shown by Brathwaite et al. (2001), scanlines that are closer to the core of vein systems are characterized by a higher mean vein thickness and a greater clustering of the veins. The presence of large fractures corresponds to the existence of major fluid drains in the rock system which can affect the development of fractures around them and thus have a great effect on the final vein distribution characteristics. In this type of hydrothermal system, the hydrothermal plume is responsible for the fluid flow directions and intensities expressed as well marked vertical and horizontal hydraulic gradients in the rock. Its location, morphology and development could therefore significantly control the spatial distribution of veins.

8. Conclusion

A statistical analyses of vein thickness in the Rosia Poieni porphyry system show that a power-law distribution exists whilst the vein spacing follows a negative exponential law. A highly clustered spatial organization of veins is suggested by both the spacing distribution and the C_v values. The final state of the vein network is representative of a saturation level in the nucleation process, as indicated by similar density values at the open-pit scale. A high probability of linkage between the veins during their growth is postulated. Veins seem to nucleate near pre-existing ones during hydrofracturing. The initial nucleation rates seem to be different and the time needed to obtain a saturation state could be shifted in time for the different levels.

A conceptual model for the development of the Rosia Poieni porphyry system in time and space is proposed. Initially, hydraulic fracturing leads to the nucleation of isolated fractures. The distribution of fluid pressure during the hydrofracturing implies different nucleation rates as a function of depth. The lower levels of the ‘‘open-pit’’ seem to exhibit a higher density of nucleation than the upper ones (Fig. 9A). It is suggested that each of these new fractures produces a specific state of stress in its vicinity allowing the nucleation of new fractures. The location of the new nucleations is therefore not random but, rather, is influenced by the initial fractures (Fig. 9B). It is suggested that the upper levels still show random new nucleation because of their initially lower nucleation rates (Fig. 9A) and that after a certain time, the saturation stage was reached in the lower levels (Fig. 9C). The existing fractures continuously grew as a function of their size and some linkage phenomena began to occur. As a result numerous veins of the same orientation develop with very low spacings, eventually coalescing to finally form some large structures. By contrast, the upper levels preserve fewer linkage phenomena and thinner thicknesses (Fig. 9D). Eventually, the saturation state was reached in the upper levels. No new nucleations occur in the entire system. The final densities of veins are similar throughout the entire ore body. The main drains are formed by linkage and favoured by the continuous growth of veins (Fig. 9E). Finally, the system stabilized as the percolation threshold was reached for the entire system. The distribution of veins is strongly clustered in the lower zones. Less clustering is observed in the upper part because of the more progressive generation of veins and the lower thicknesses of the last generation of veins (Fig. 9F).

Acknowledgements

This research was carried out within the French Metallogeny ‘‘GdR Transmet’’ research program. The authors would like to thank the Geological Institute of Romania (IGR) and ‘‘Regia Autonoma de Cupru’’ for their field support and permission to access the Rosia Poieni open-pit. Thanks are also addressed to L. Bailly, M. Lespinasse, S. Udubasa, L. Grancea, J.L. Leroy and V. Milu for their valuable help during the field work.

We also thank P. Gillespie and an anonymous reviewer for their constructive reviews, and finally the editor Bob Holdsworth for a thorough and professional editing of this article.

References

Alderton, D.H.M., Thirlwall, M.F., Baker, J.A., 1998. Hydrothermal alteration associated with gold mineralization in the southern Apuseni Mountains, Romania: preliminary Sr isotopic data. Mineralium Deposita 33, 520–523.

Barton, C.A., Zobach, M.D., 1990. Self-similar distribution of macroscopic fractures at depth in crystalline rock in the Cajon Pass scientific drill hole. In: Barton, N., Stephansson, O. (Eds.), Rock Joints. Balkema, Rotterdam, pp. 163–170.

Berkowitz, B., Adler, P.M., 1998. Stereological analysis of fracture network structure in geological formations. Journal of Geophysical Research B103, 15,339.

Bodnar, R.J., 1995. Fluid inclusion evidence for a magmatic source of metals in porphyry copper deposits. In: Thompson, J.F.H. (Ed.), Magmas, Fluids, and Ore Deposits. Mineralogical Association of Canada Short Courses Series, vol. 23, pp. 139–152 (Victoria).

Borcos, M., Kräutner, H.G., Udubasa, G., Sandulescu, M., Nastaseanu, S., Bitoianu, C., 1983. Map of Mineral Resources of Romania. Institute of Geology and Geophysics, Bucarest.

Bostinescu, S., 1984. Porphyry copper systems in the south Apuseni Mountains – Romania. Ann. I.G.R. LXIV, 163–175.

Bonnet, E., Bour, O., Odling, N., Davy, P., Main, I., Cowie, P., Berkowitz, B., 2001. Scaling of fracture systems in geological media. Reviews of Geophysics 39 (3), 347–383.

Borcos, M., Vlad, S., Udubasa, G., Gabudeanu, B., 1998. Qualitative and quantitative metallogenetic analysis of the ore genetic units in Romania. Romanian Journal of Mineral Deposits 78, 1–83.

Bour, O., Davy, P., Darcel, C., 2002. A statistical scaling model for fracture network geometry, with validation on a multiscale mapping of a joint network (Hornelen Basin, Norway). Journal of Geophysical Research 107.

Bour, O., Davy, P., 1999. Clustering and size distributions of fault patterns: theory and measurements. Geophysical Research Letters 26, 2001–2004.

Brathwaite, R.L., Cargill, H.J., Christie, A.B., Swain, A., 2001. Lithological and spatial controls on the distribution of quartz veins in andesite- and rhyolite-hosted epithermal Au–Ag deposits of the Hauraki Goldfield, New Zealand. Mineralium Deposita 36, 1–12.

Brooks, B.A., Allmendinger, R.W., Garrido de la Barra, I., 1996. Fault spacing in the El Teniente Mine, central Chile: evidence for nonfractal fault geometry. Journal of Geophysical Research 101 (B6), 13633–13653.

Cartwright, J.A., Trufgill, B.D., Mansfield, C.S., 1995. Fault growth by segment linkage: an explanation for scatter in maximum displacement and trace length data from the Canyonlands Grabens of SE Utah. Journal of Structural Geology 17, 1319–1326.

Cioflica, G., Savu, H., Borcos, M., Stefan, A., Istrate, G., 1973. Alpine volcanism and metallogenesis in the Apuseni Moutains. In the Symposium: Volcanism and Metallogenesis. Guide Books. Geological Institute of Bucharest, Bucharest. 71.

Clark, M.B., Brantley, S.L., Fisher, D.M., 1995. Power-law vein-thickness distributions and positive feedback in vein growth. Geology 23, 975–978.

Cowie, P.A., Malinverno, A., Ryan, W.B.F., Edwards, M.H., 1994. Quantitative fault studies on the East Pacific Rise: a comparison of sonar imaging techniques. Journal of Geophysical Research 99 (B8), 15205–15218.

Cox, D.R., Lewis, P.A.W., 1966. The Statistical Analysis of Series of Events. Methuen, London.

Cox, S.F., 1999. Deformational controls on the dynamics of fluid flow in mesothermal gold systems. In: Mc Caffrey, K.J.W., Lonergan, L., Wilkinson, J.J. (Eds.), Fractures, Fluid Flow and Mineralization, vol. 155. Geological Society Special Publications, London, pp. 123–140.

Genter, A., Traineau, H., Dezayes, C., Elsass, P., Ledésert, B., Meunier, A., Villemin, T., 1995. Fracture analysis and reservoir characterization of the granitic basement in the HDR Soultz project (France). Geothermal Science and Technology 4 (3), 189–214.

Gillespie, P.A., Walsh, J.J., Watterson, J., 1992. Limitations of dimension and displacement data from single faults and the consequences for data analysis and interpretation. Journal of Structural Geology 14, 1157–1172.

Gillespie, P.A., Howard, C., Walsh, J.J., Watterson, J., 1993. Measurement and characterisation of spatial distributions of fractures. Tectonophysics 226, 113–141.

Gillespie, P.A., Johnston, J.D., Loriga, M.A., Mc Caffrey, K.J.W., Walsh, J.J., Watterson, J., 1999. Influence of layering on vein systematics in line samples. In: Mc Caffrey, K.J.W., Lonergan, L., Wilkinson, J.J. (Eds.), Fractures, Fluid Flow and Mineralization, vol. 155. Geological Society Special Publications, London, pp. 35–56.

Gillespie, P.A., Walsh, J.J., Watterson, J., Bonson, C.G., Manzocchi, T., 2001. Scaling relationships of joint and vein arrays from the Burren Co. Clare, Ireland. Journal of Structural Geology 23, 183–201.

Gross, M.R., Engelder, T., 1995. Strain accommodated by brittle failure in adjacent units of the Monterey Formation, USA: scale effects and evidence for uniform displacement boundary conditions. Journal of Structural Geology 17, 1303–1318.

Harris, C., Franssen, R., Loosveld, R., 1991. Fractal analysis of fractures in rocks: the Cantor's Dust method – comment. Tectonophysics 198, 107–115.

Hedenquist, J.W., Lowenstern, J.B., 1994. The role of magmas in the formation of hydrothermal ore deposits. Nature 370, 519–527.

Heinrich, C.A., Neubauer, F., 2002. Cu–Au–Pb–Zn–Ag metallogeny of the Alpine–Balkan–Carpathian–Dinaride geodynamic province. Mineralium Deposita 37, 533–540.

Ianovici, V., Vlad, S., Borcos, M., Bostinescu, S., 1977. Alpine porphyry copper mineralization of West Romania. Mineralium Deposita 12, 307–317.

Ijiri, Y., Simons, H., 1977. Skew Distributions and the Sizes of Business Firms. North Holland Publishing Company, Amsterdam.

Ionescu, O., 1974. Mineralizatia cuprifera de tip diseminat de la Rosia Poieni (jud. Alba). St Cerc. Geol. Geof. Geogr. 19, 77–84.

Ionescu, O., Soare, C., Gherghiu, 1975. Contributii la cunoasterea zacamantulu Rosia Poieni (Muntii Metaliferi), Alteratii hipogene. St Cerc. Geol. Geof. Geogr. 20, 159–170.

Johnston, J.D., 1992. The fractal geometry of vein systems: the potential for ore reserve calculation. In: Bowden, A.A., Earls, G., O'Connor, P.G., Pyne, J.F. (Eds.), The Irish Minerals Industry 1890–1990. Irish Association for Economic Geology, pp. 105–117.

Johnston, J.D., Mc Caffrey, J.W., 1996. Fractal geometry of vein systems and the variation of scaling relationships with mechanism. Journal of Structural Geology 18, 349–358.

Khrul, J.H., 1994. The formation of extensional veins: an application of the control dust model. In: Khrul, J.H. (Ed.), Fractals and Dynamic Systems in Geoscience. Springer, Berlin, pp. 95–104.

La Pointe, P.R., 1988. A method to characterize fracture density and connectivity through fractal geometry. International Journal of Rock Mechanics and Mining Sciences and Geomechanical Abstracts 25, 421–429.

Ledésert, B., Dubois, J., Genter, A., Meunier, A., 1993a. Fractal analysis of fractures applied to Soultz-sous-Forets hot dry rock geothermal program. Journal of Volcanology and Geothermal Research 57, 1–17.

Ledésert, B., Dubois, J., Velde, B., Meunier, A., Genter, A., Badri, A., 1993b. Geometrical and fractal analysis of a three-dimensional hydrothermal vein network in a fractured granite. Journal of Volcanology and Geothermal Research 56, 267–280.

Lemne, M., Vidjea, E., Borcos, M., Tanasescu, A., Romanescu, O., 1983. Des datations K–Ar concernant les magmatites subséquentes alpines des Monts Apuseni. Anuarul Institului Geologie Geofizica 61, 375–386.

Long, J.C.S., Witherspoon, P.A., 1985. The relationship of the degree of interconnection to permeability in fracture networks. Journal of Geophysical Research 90 (B4), 3087–3098.

Loriga, M.A., 1999. Scaling systematics of vein size: an example from the Guanajuato mining district (Central Mexico). In: Mc Caffrey, K.J.W., Lonergan, L., Wilkinson, J.J. (Eds.), Fractures, Fluid Flow and Mineralization, vol. 155. Geological Society Special Publications, London, pp. 57–67.

Mandelbrot, B.B., 1983. The Fractal Geometry of Nature. Freeman, New York.

Mc Caffrey, K.J.W., Johnston, J.D., 1996. Fractal analysis of a mineralised vein deposit: Cuurraghinalt gold deposit County Tyrone. Mineralium Deposita 31, 52–58.

Merceron, T., Velde, B., 1991. Application of Cantor's method for fractal analysis of fractures in the Toyoha mine, Hokkaïdo, Japan. Journal of Geophysical Research 96 (B10), 16641–16650.

Milu, V., 1999. Alteratii hidrotermale asociate zacamintelor de tip porphyry copper Bolcana si Rosia Poieni (Muntii Apuseni de Sud), Thèse de l'Université de Bucarest.

Milu, V., Milési, J.P., Leroy, J.L., 2004. Rosia Poieni copper deposit, Apuseni Mountains, Romania: advanced argillic overprint of a porphyry system. Mineralium Deposita 39, 173–188.

Monecke, T., Gemmell, J.B., Monecke, J., 2001. Fractal distributions of veins in drill core from the Hellyer VHMS deposit, Australia: constraints on the origin and evolution of the mineralising system. Mineralium Deposita 36, 406–415.

Narr, W., Suppe, J., 1991. Joint spacing in sedimentary rocks. Journal of Structural Geology 13, 1037–1048.

Park, H.J., West, T.R., 2002. Sampling bias of discontinuity orientation caused by linear sampling technique. Engineering Geology 66, 99–110.

Peacock, D.C.P., Harris, S.D., Mauldon, M., 2003. Use of curved scanlines and boreholes to predict fracture frequencies. Journal of Structural Geology 25, 109–119.

Pecksay, Z., Edelstein, O., Seghedi, I., Szakacs, A., Kovacs, M., Crihan, M., Bernad, A., 1995. K–Ar datings of Neogene-Quaternary calk-alkaline volcanic rocks in Romania. Acta Vulcanologica 7 (2), 53–61.

Pickering, G., Bull, J.M., Sanderson, D.J., 1995. Sampling power-law distributions. Tectonophysics 248, 1–20.

Priest, S.D., Hudson, J.A., 1976. Discontinuity spacings in rock. International Journal of Rock Mechanics and Mining Sciences and Geomechanical Abstracts 13, 135–148.

Rives, T., Razack, M., Petit, J.P., Rawnsley, K.D., 1992. Joint spacing: analogue and numerical simulations. Journal of Structural Geology 14 (8/9), 925–937.

Roberts, S., Sanderson, D.J., Gumiel, P., 1998. Fractal analysis of Sn–W mineralization from central Iberia: insights into the role of fracture connectivity in the formation of an ore deposit. Economic Geology 93, 360–365.

Roberts, S., Sanderson, D.J., Gumiel, P., 1999. Fractal analysis and percolation properties of veins. In: Mc Caffrey, K.J.W., Lonergan, L., Wilkinson, J.J. (Eds.), Fractures, Fluid Flow and Mineralization, vol. 155. Geological Society Special Publications, London, pp. 7–16.

Rosu, E., Pecskay, Z., Stefan, A., Popescu, G., Panaiotu, C., Panaiotu, C.E., 1997. The evolution of the Neogene volcanism in the Apuseni Mountains (Rumania): Constraints from new K–Ar data. Geologica Carpathica 48 (6), 353–359.

Sanderson, D.J., Roberts, S., Gumiel, P., 1994. A fractal relationship between vein thickness and gold grade in drill core from La Codosera, Spain. Economic Geology 89, 168–173.

Simpson, G.D.H., 2000. Synmetamorphic vein spacing distributions: characterisation and origin of veins from NW Sardinia, Italy. Journal of Structural Geology 22, 335–348.

Smalley, R.F., Chatelain, J.L., Turcotte, D.L., Prevot, R., 1987. A fractal approach to the clustering of earthquakes: applications to the seismicity of the New Hebrides. Bulletin of Seismological Society of America 77, 1368–1381.

Terzaghi, R.D., 1965. Sources of error in joint surveys. Geotechnique 15 (3), 287–304.

Udubasa, G., Strusievicz, R., Dafin, E., Verdes, G., 1992. Mineral occurrences in the Metaliferi Mountains, Romania. Romanian Journal of Mineralogy 75 (2), 35.

Velde, B., Dubois, J., Touchard, G., Badri, A., 1990. Fractal analysis of fractures in rocks: the Cantor's Dust method. Tectonophysics 179, 345–352.

Velde, B., Dubois, J., Moore, D., Touchard, G., 1991. Fractal patterns of fractures in granites. Earth and Planetary Science Letters 104, 23–35.

Wilkinson, J.J., Johnston, J.D., 1996. Pressure fluctuation, phase separation, and gold precipitation during seismic fracture propagation. Geology 24, 395–398.